Turbulent Viscous-Shock-Layer Solutions with Strong Vorticity Interaction

E. Clay Anderson,*
DCW Industries, Sherman Oaks, Calif.

James N. Moss,† and Kenneth Sutton†
NASA Langley Research Center, Hampton, Va.

Numerical solutions of the viscous-shock-layer equations governing laminar and turbulent flows of a perfect gas and mixtures of perfect gases in chemical equilibrium are presented for hypersonic flow over spherically blunted cones and hyperboloids. The results are compared with boundary-layer and inviscid flowfield solutions. The agreement with the inviscid flowfield data is satisfactory. The agreement with boundary-layer solutions is good except in regions of strong vorticity interaction. In these flow regions, the viscous-shock-layer solutions appear to be more satisfactory than the boundary-layer solutions.

Nomenclature

C_i = mass fraction of species i, ρ_i/ρ
C_ℓ = mass fraction of element ℓ
C_p = frozen specific heat of mixture $\sum_{i=1}^{N} C_i C_{p,i}$
$C_{p,i}$ = specific heat of species i, $C^*_{p,i}/C^*_{p,\infty}$
H = defined quantity, $h+(u^2/2)$
H_t = total enthalpy $H+(v^2/2)$
h = enthalpy of mixture, $\sum_{i=1}^{N} C_i h_i$
h_i = enthalpy of species i, h^*_i/U^{*2}_∞
j = flow index: 0 for plane flow; 1 for axisymmetric flow
K = thermal conductivity of mixture, $K^*/\mu^*_{\text{ref}} C^*_{p,\infty}$
M^* = molecular weight
$\bar{M}^*$ = molecular weight of mixture
N = number of species
N_{Le} = Lewis number, $\rho^* D^*_{ij} C^*_p/K^*$
$N_{Le,T}$ = turbulent Lewis number
N_{Pr} = Prandtl number, $\mu^* C^*_p/K^*$
$N_{Pr,T}$ = turbulent Prandtl number, $\mu^*_T C^*_p/K^*_T$
N_{Re} = Reynolds number, $\rho^*_\infty U^*_\infty r^*_n/\mu^*_\infty$
N_{Sc} = Schmidt number, $N_{Sc}=N_{Pr}/N_{Le}$
n = coordinate measured normal to body, n^*/r^*_n
p = pressure, $p^*/[\rho^*_\infty (U^*_\infty)^2]$
$-q_{c,w}$ = convective heat flux to the wall [Eq. (7)]
r = radius measured from axis of symmetry to point on body surface, r^*/r^*_n
r^*_n = nose radius
s = coordinate measured along body surface, s^*/r^*_n
T = temperature, T^*/T^*_{ref}
T^*_{ref} = temperature $(U^*_\infty)^2/C^*_{p,\infty}$
U^*_∞ = freestream velocity
u = velocity component tangent to body surface, u^*/U^*_∞
v = velocity component normal to body surface, v^*/U^*_∞
α = shock angle defined in Fig. 1
δ = boundary-layer thickness
$\delta_{i\ell}$ = number of atoms of the ℓth element in species i
ϵ^+ = normalized eddy viscosity, μ_T/μ
η = transformed n-coordinate, n/n_s
θ = body angle defined in Fig. 1
κ = body curvature
μ = molecular viscosity, $\mu^*/\mu^*(T^*_{\text{ref}})$
μ_T = eddy viscosity
ξ = coordinate measured along body surface, $\xi=s$
ρ = density of mixture, ρ^*/ρ^*_∞
σ = Reynolds number parameter $[\mu^*(T^*_{\text{ref}})/\rho^*_\infty U^*_\infty r^*_n]^{1/2}$
$\phi_{1,2,3}$ = quantities defined by Eqs. (4b, 4c, 4d)

Superscripts

j = 0 for plane flow; 1 for axisymmetric flow
$*$ = dimensional quantity
$''$ = shock-oriented velocity component (see Fig. 1)

Subscripts

e = boundary-layer edge
i = ith species
ℓ = ℓth element
s = shock
w = wall
∞ = freestream

Presented as Paper 76-120 at the AIAA 14th Aerospace Sciences Meeting; Washington, D.C., Janurary 26-28, 1976; submitted April 26, 1976; revision received Oct. 4, 1976.

Index categories: Boundary Layers and Convective Heat Transfer – Turbulent; Supersonic and Hypersonic Flow.

*Consulting Engineer.

†Research Engineer. Member AIAA.

Introduction

VORTICITY interaction between the boundary layer and the outer inviscid entropy layer is not significant for high Reynolds number laminar flows over blunt bodies having low angle afterbodies except at distances far downstream. However, for large angle afterbodies such as those being considered for planetary entry probes,[1] vorticity interaction is strong in the region near the nose of the body if the flow is turbulent and can be a significant influence for laminar flows if mass injection is considered.

The use of higher-order boundary-layer theory for the analysis of flowfields with a high degree of coupling between the boundary layer (BL) and the inviscid flow requires a complex iterative solution procedure. Because of the difficulties experienced in the application of higher order BL theory, Davis[2,3] has developed a numerical technique for solving the viscous-shock-layer (VSL) equations governing laminar flow of a perfect gas and for binary mixtures with finite rate chemical reactions. Moss[4] has developed VSL solutions for multicomponent gas mixtures for both equilibrium and finite rate chemistry. Moss[5] has extended the equilibrium chemistry analysis to include the effects of radiation heat transfer. These VSL analyses have been found accurate for flows with strong vorticity interaction and/or radiation heat transfer.

In recent publications by Eaton and Larson[6] and Anderson and Moss,[7] numerical solutions of the VSL equations governing turbulent flow of a perfect gas have been presented. Eaton and Larson considered the thin VSL equations and presented solutions for turbulent flow over slender cones. Their results were compared with experimental data and showed good agreement. Anderson and Moss considered turbulent flow over blunt axially symmetric bodies and used the full VSL equations. These solutions were compared with first-order turbulent BL theory. The results obtained with this turbulent VSL analysis were essentially identical to first-order turbulent BL results in the region where vorticity interaction is not significant. For the downstream region, the expected differences were obtained.

In a later investigation, Anderson and Moss[8] extended the turbulent VSL analysis to reacting gas mixtures in chemical equilibrium and considered both radiating and nonradiating shock layers. These turbulent VSL solutions were compared with first-order BL solutions and first-order BL theory with corrections for streamline swallowing (BLSSW). A nonradiating shock-layer solution corresponding to a typical trajectory point for a Venusian entry was considered. A cold-wall boundary condition was assumed, and the results of the VSL analysis were compared with integral BL and BLSSW analyses. The two BL solutions and the VSL solution showed excellent agreement in the laminar flow region. For the turbulent flow region, both the BLSSW and the VSL solution showed a large increase in the heat-transfer rate when compared with the BL solution. For the turbulent flow region, the VSL heat-transfer rates were 14% to 30% lower than the solution obtained with the integral BLSSW anslysis, but the general trend in the heat-transfer rate distribution was the same for both methods of analysis.

For the more complex case of a radiating shock layer with mass injection at the surface, a typical trajectory point for a Venus entry was analyzed. These VSL results were compared with an integral matrix BLSSW analysis. For this case, the laminar flow region solutions differed by 10% to 15% in convective heating-rate predictions, and for the turbulent flow region, the two methods of analysis showed opposite trends in the convective-heating-rate distribution. The BLSSW analysis predicted a maximum convective heating rate at the transition point. The VSL analysis predicted the maximum convective heating rate at a downstream location. For the predominantly inviscid outer flow region of the shock layer, the VSL solution was found to be in satisfactory agreement with the inviscid flowfield solution. The prediction of radiation heating at the surface was in satisfactory agreement with the BLSSW analysis.

The opposite trends in the calculated convective heating-rate distributions appeared to be the result of an increase in vorticity interaction caused by mass injection and the higher temperature at the surface boundary. This behavior was not obtained for the nonradiating case with no injection and cold-wall boundary conditions. The cold-wall boundary condition results in a thinner BL thickness and diminishes the influence of vorticity interaction. Both higher surface temperature and mass injection increase vorticity interaction.

The present investigation is directed primarily toward determining the behavior of BLSSW and VSL solutions in regions of strong vorticity interaction. To reduce the number of variables to a minimum, a perfect gas is considered, and eddy viscosity modeling techniques are identical in both the VSL and BLSSW analyses. Representative VSL profile data are compared with two different inviscid flowfield solutions and BL and BLSSW solutions. VSL solutions are also presented for mixtures of perfect gases in chemical equilibrium.

Analysis

Governing Equations

The equations of motion for reacting gas mixtures in chemical equilibrium are presented by Bird, Stewart, and Lightfoot.[9] The formulation of these equations in body-oriented coordinates appropriate for VSL analysis of laminar flow of radiating and nonradiating gases in presented by Moss.[4,5]

For turbulent flow, the VSL equations are derived using methods analogous to those presented by Dorrance[10] for the turbulent-boundary-layer equations and are expressed in nondimensional for for the coordinate system shown in Fig. 1 as

Continuity:

$$\frac{\partial}{\partial s}\left[(r+n\cos\theta)^{j}\rho u\right]+\frac{\partial}{\partial n}\left[(1+n\kappa)(r+n\cos\theta)^{j}\rho v\right]=0 \quad (1)$$

s-momentum:

$$\rho\left(\frac{u}{1+n\kappa}\frac{\partial u}{\partial s}+v\frac{\partial u}{\partial n}+\frac{uv\kappa}{1+n\kappa}\right)+\frac{1}{1+n\kappa}\frac{\partial p}{\partial s}$$
$$=\sigma^{2}\left\{\frac{\partial}{\partial n}\left[\mu(1+\epsilon^{+})\frac{\partial u}{\partial n}-\frac{\mu u\kappa}{1+n\kappa}\right]\right.$$
$$\left.+\left(\frac{2\kappa}{1+n\kappa}+\frac{j\cos\theta}{r+n\cos\theta}\right)\left[\mu(1+\epsilon^{+})\frac{\partial u}{\partial n}-\frac{\mu u\kappa}{1+n\kappa}\right]\right\} \quad (2)$$

n-momentum:

$$\rho\left(\frac{u}{1+n\kappa}\frac{\partial v}{\partial s}+v\frac{\partial v}{\partial n}-\frac{u^{2}\kappa}{1+n\kappa}\right)+\frac{\partial p}{\partial n}=0 \quad (3)$$

Energy:

$$\rho\left(\frac{u}{1+n\kappa}\frac{\partial H}{\partial s}+v\frac{\partial H}{\partial n}\right)-v\frac{\partial p}{\partial n}+\frac{\rho u^{2}v\kappa}{1+n\kappa}$$
$$=\sigma^{2}\left[\frac{\partial}{\partial n}(\phi_{1}+\phi_{2}+\phi_{3})\right.$$
$$\left.+\left(\frac{\kappa}{1+n\kappa}+\frac{j\cos\theta}{r+n\cos\theta}\right)(\phi_{1}+\phi_{2}+\phi_{3})\right] \quad (4a)$$

where

$$\phi_{1}=\frac{\mu}{N_{Pr}}\left(1+\epsilon^{+}\frac{N_{Pr}}{N_{Pr,T}}\right)\frac{\partial H}{\partial n} \quad (4b)$$

$$\phi_{2}=\frac{\mu}{N_{Pr}}\left[N_{Pr}-1+\frac{\epsilon^{+}N_{Pr}}{N_{Pr,T}}(N_{Pr,T}-1)\right]u\frac{\partial u}{\partial n}-\frac{\mu u^{2}\kappa}{1+n\kappa} \quad (4c)$$

$$\phi_{3}=\frac{\mu}{N_{Pr}}\left[N_{Le}-1+\epsilon^{+}\frac{N_{Pr}}{N_{Pr,T}}(N_{Le,T}-1)\right]\sum_{i=1}^{N}h_{i}\frac{\partial C_{i}}{\partial n} \quad (4d)$$

and

$$H\equiv h+(u^{2}/2) \quad (4e)$$

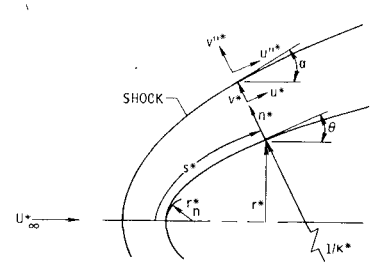

Fig. 1 Coordinate system.

Elemental continuity:

$$\rho\left(\frac{u}{1+n\kappa}\frac{\partial\tilde{C}_\ell}{\partial s}+\frac{v\partial\tilde{C}_\ell}{\partial n}\right)=\frac{\sigma^2}{(1+n\kappa)(r+n\cos\theta)^j}$$

$$\times\frac{\partial}{\partial n}\left\{\left[(1+n\kappa)(r+n\cos\theta)^j\frac{\mu}{N_{Pr}}\left(N_{Le}+\epsilon\frac{N_{Pr}}{N_{Pr,T}}N_{Le,T}\right)\frac{\partial\tilde{C}_\ell}{\partial n}\right]\right\} \tag{5a}$$

where

$$\tilde{C}_\ell=\sum_{i=1}^{N}\delta_{i_\ell}\frac{M^*_\ell}{M^*_i}C_i \tag{5b}$$

State:

$$p=\rho TR^*/\bar{M}^*C^*_{p,\infty} \tag{6}$$

Boundary Conditions

The boundary conditions at the shock are calculated by using the Rankine-Hugoniot relations. At the wall, the no-slip and no-temperature-jump boundary conditions are used; consequently, $u_w=0$. The wall temperature and mass injection rate are either specified or calculated. For the calclated mass injection conditions, the ablation process is assumed to be quasi-steady and the wall temperature is the sublimation temperature of the ablator surface.

The heat transferred to the wall due to conduction and diffusion is

$$-q_{c,w}=\sigma^2\left(K\frac{\partial T}{\partial n}+\frac{\mu}{N_{Sc}}\sum_{i=1}^{N}h_i\frac{\partial C_i}{\partial n}\right)_w \tag{7}$$

More complete boundary conditions are presented in Ref. 11.

Thermodynamic and Transport Properties

The equilibrium composition is determined by a free energy minimization calculation.[12] Thermodynamic properties for specific heat, enthalpy, and free energy and transport properties for viscosity and thermal conductivity are required for each species considered. Values for the thermodynamic[13,14] and transport properties[15] are obtained by using polynomial curve fits. The mixture viscosity is obtained by using the semiempirical formula of Wilke.[16]

Eddy-Viscosity Approximations

A two-layer eddy-viscosity model consisting of an inner law based upon Prandtl's mixing'length concept and the Clauser-Klebanoff expression (based on Refs. 17 and 18) for the outer law is used in the present investigation. This model, introduced by Cebeci,[19] assumes that the inner law is applicable for the flow from the wall out to the location where the eddy viscosity given by the inner law is equal to that of the outer law. The outer law is then assumed applicable for the remainder of the viscous layer. It is noted that the eddy viscosity degenerates to approximately zero in the inviscid portion of the shock layer. The degeneracy is expressed in terms of the normal intermittency factor given by Klebanoff.[18]

This model requires a definition of the boundary-layer thickness δ which is assumed to be the value of n at the point where

$$H_t/H_{t,\infty}=0.995 \tag{8}$$

and is defined by linear interpolation in an array of local total enthalpies. This definition is approximately equivalent to the usual boundary-layer definition

$$u/u_e=0.995 \tag{9}$$

where u_e is the local value for the undisturbed inviscid flow outside the boundary layer. For the present study, the turbulent Prandtl and Lewis numbers are assumed to be 0.9 and 1.0, respectively.

Method of Solution

Davis[2] presented a method for solving the VSL equations for stagnation and downstream flow. Moss[4,5] applied this method of solution to reacting multicomponent mixtures. The present method of solution is identical to that of Refs. 2 and 4. Therefore, the solution procedure is not presented here.

Results and Discussion

Numerical solutions of the VSL equations governing laminar, transitional, and turbulent flows of a perfect gas are compared with inviscid, BL, and BLSSW solutions. Equivalent but less extensive comparisons are presented for nonradiating mixtures of perfect gases in chemical equilibrium.

Perfect Gas Solutions with Strong Vorticity Interaction

VSL solutions for laminar and turbulent flow of a Mach 10 freestream over a 40° half-angle spherically blunted cone are presented. Representative profile data obtained using the VSL analysis are compared with inviscid, BL, and BLSSW profile data. The inviscid flowfield solutions were obtained using the blunt-body method of characteristics (MOC) of Inouye et al.[20] and the transient finite-difference (TFD) procedure of Sutton.[21] The BL data were obtained using the analysis of Anderson and Lewis.[22] BLSSW data were obtained using the analysis of Mayne and Dyer[23] (this solution was provided by A. W. Mayne Jr. of ARO, Inc.), and the analysis of Ref. 22 was modified to account for variable entropy edge conditions during the present investigation.

Surface pressure distributions corresponding to the VSL and MOC solutions are shown in Fig. 2. Excellent agreement is obtained except in the vicinity of the sphere-cone tangency point where differences are ±10%. These differences have little influence upon the downstream flow and are not excessive in the region near the tangency point. The shock shapes corresponding to the VSL and MOC solutions are essentially identical and are not presented.

Figure 3 shows heating-rate distributions corresponding to: 1) the BL analysis of Ref. 22, 2) the BLSSW analysis of Ref. 23, 3) VSL solutions corresponding to the assumptions that the BL edge is located as defined by Eq. (8) and at the bow shock, and 4) laminar VSL and BLSSW[22] solutions. For turbulent flow, instantaneous transition at $s=0.8$ has been assumed.

The turbulent VSL solution with the BL edge location defined by Eq. (8) and using Kelbanoff's normal intermittency factor is in excellent agreement with the BL anslysis of Ref. 22 for $s\leq 2.5$. In the region of strong vorticity interaction, the heating rates predicted by the VSL solution are as much as 40% less than the heating rates predicted by the two BLSSW solutions. In the downstream region where the inviscid entropy layer has been swallowed by the BL, and VSL and BLSSW solutions approach an equivalent cone solution, as they should.

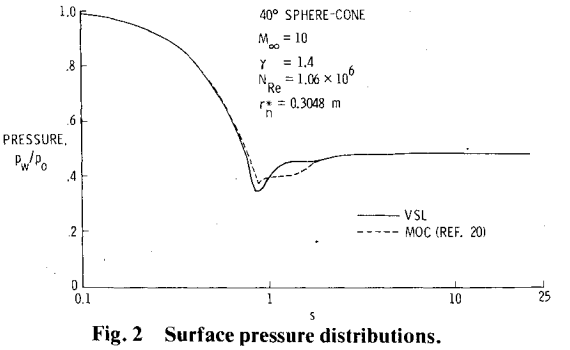

Fig. 2 Surface pressure distributions.

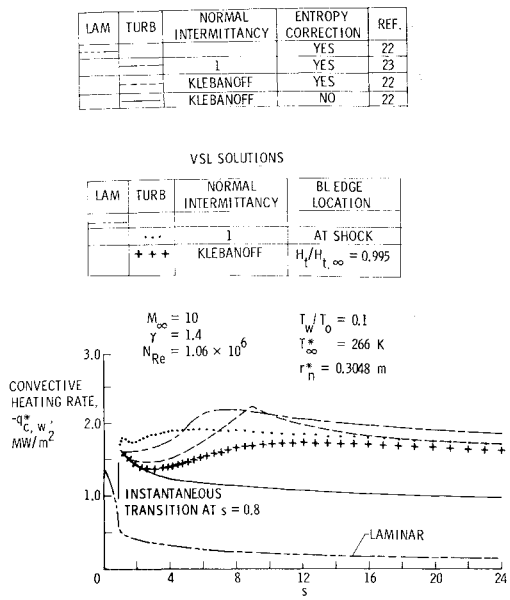

Fig. 3 Heating-rate distributions.

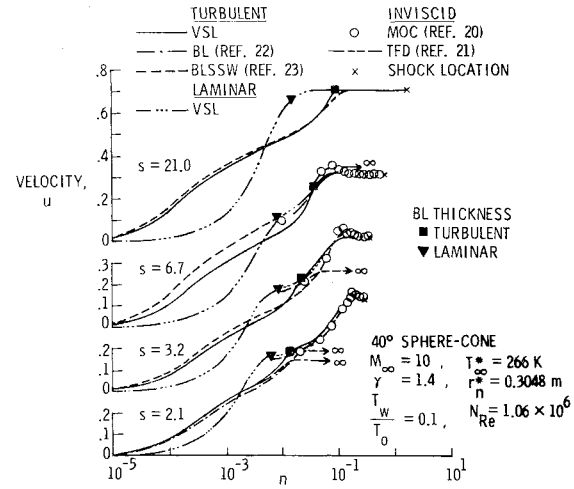

Fig. 4 Comparisons of velocity profiles.

The turbulent VSL solution is strongly influenced by the definition of the BL edge location. To demonstrate the maximum influence of the BL edge definition on the VSL solution, the BL edge was assumed to be located at the bow shock and a unit value for Klebanoff's normal intermittency factor was assumed. These assumptions result in maximum eddy viscosities using the present mixing length turbulence model. This solution shows the expected behavior, but the peak heating rates predicted by the VSL solution remains substantially less than that given by the BLSSW solutions. The laminar VSL and BLSSW[22] solutions which are not directly influenced by the BL and the displacement thicknesses show excellent agreement (±3%) for the heating-rate distribution. The data presented are the VSL solution.

The apparent contradiction for the agreement between laminar and turbulent VSL and BLSSW solutions is the result of the BL and the displacement thickness distributions obtained using the BLSSW analyses. Both BLSSW solutions showed a linear increase in the BL and the displacement thickness distributions up to the point where the inviscid entropy layer is swallowed by the BL. Downstream of this point, these thickness distributions showed a gradual decrease in magnitude until the equivalent cone solution was approached. Since these definitions determine the scale for turbulence, the turbulent-heating-rate distributions predicted by the BLSSW solutions show the same behavior.

The rapid growth of the BL and displacement thickness in the region where longitudinal entropy gradients were significant was obtained for both laminar and turbulent flow when the variable entropy corrections presented by Blottner[24] were used in the analysis of Ref. 22. An approximate streamline swallowing analysis which corrected only the edge conditions was also used. This approach has been used by Price and Harris[25] and was found to give a more satisfactory distribution for the BL and the displacement thicknesses. The heat-transfer-rate distribution obtained with this approximate analysis was essentially the same as when the full modifications presented by Blottner[24] were used. A more accurate BL solution would require higher-order theory (see van Dyke[26]).

Figure 4 shows velocity profile data at four locations. The VSL solutions are compared with the inviscid flowfield solutions of Refs. 20 and 21, the BLSSW solution of Ref. 23, and the BL solution of Ref. 22. At $s=2.1$, the VSL profile data in the inner viscous region shows good agreement with both the BL and BLSSW solutions for turbulent flow. However, as is evident from the different heating rates predicted at this station, the temperature profiles corresponding to the BLSSW solution showed pronounced differences from that of the VSL solution. The temperature profiles corresponding to the BL solution show good agreement with the VSL solution as indicated by the heating-rate prediction. These data are not presented.

In the predominantly inviscid outer flow region, the VSL profile data show satisfactory agreement (±5%) with both inviscid flowfield solutions. The VSL and TFD solutions do not show the distinct sharp peak in the velocity profile that is a characteristic of spherically blunted cone flowfields as shown by the MOC results. Since TFD inviscid flowfield solutions generally use less than 15 interior grid points across the shock layer, the differences between the TFD and MOC solutions are probably the result of inadequate resolution. The VSL solutions were obtained using 150 interior grid points with approximately 80 points within the predominantly viscous inner region and the remaining 70 points in the predominantly inviscid outer region. Since velocity and temperature gradients are relatively large in the inviscid entropy layer, the differences between the MOC and VSL solutions appear to be the result of viscous and displacement effects.

Profile data at $s=3.2$ and 6.7 show that the agreement between the VSL and BLSSW solution becomes progressively worse as vorticity increases at the BL edge. After the inviscid entropy layer is swallowed by the viscous layer, the agreement between the two methods of solution is satisfactory as shown at $s=21$. The profile data at $s=6.7$ show that the inviscid entropy layer has been swallowed by the BL using the BLSSW analysis. The VSL profile data show a distinct "inviscid entropy layer," and these data are in satisfactory agreement with both inviscid flowfield solutions.

The solutions presented for the 40° half-angle spherically blunted cone indicate that the VSL solution procedure is satisfactory for high Reynolds number laminar and turbulent flows. The VSL solutions using algebraic mixing length turbulence models in conjunction with the definition expressed by Eq. (8) for the BL edge location show acceptable agreement with BL solutions in the nose region of blunt bodies and with BLSSW solutions in the far downstream flow. The VSL solutions appear to be more satisfactory than BLSSW solutions for flows with strong vorticity interaction. However, the accuracy of the present solution procedure and the applicability of the algebraic mixing length turbulence modeling technique in the presence of strong vorticity interaction must be determined by experimental verification. Turbulence models which are independent of conventional boundary-layer thickness definitions are needed for the present method of analysis.

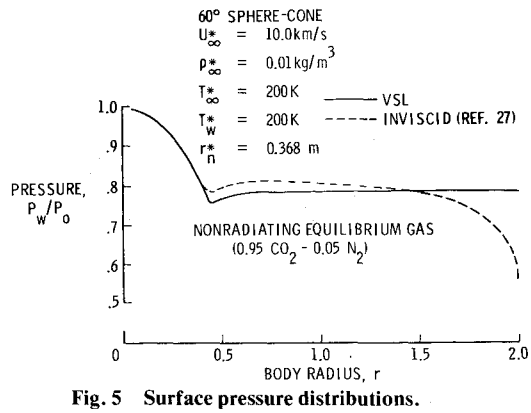

Fig. 5 Surface pressure distributions.

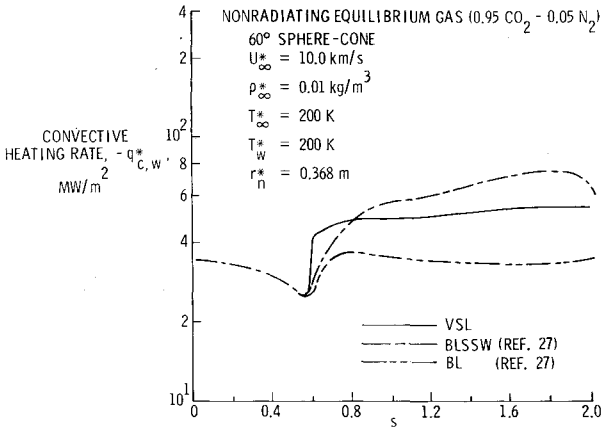

Fig. 6 Heating-rate distributions.

Solutions for Perfect Gas Mixtures in Chemical Equilibrium

A VSL solution for the flowfield over a 60° half-angle spherically blunted cone for a typical Venusian entry trajectory point is presented in Figs. 5 and 6. The VSL solution is compared with BL and BLSSW solutions obtained using the integral analysis of Edquist[27] (this solution was provided by C.T. Edquist, Martin-Marietta Corp., Denver Division).

The inviscid flowfield solution used to specify edge conditions for the BL and BLSSW solutions was determined using a single strip integral method which accounts for the upstream influence of the sonic corner. The present formulation of the VSL equations cannot account for this influence. The surface pressure distributions corresponding to the two methods of analysis are shown in Fig. 5. The influence of the sonic corner is significant only in the region $1.6 \leq r < 2$. For $r \leq 1.6$, the maximum difference between the two methods of analysis is less than 4%.

Convective heat-transfer rate distributions corresponding to the integral BL and BLSSW solutions and the present VSL solution are presented in Fig. 6. The present solution corresponds to assuming instantaneous transition from laminar to turbulent flow with Eq. (8) used for the BL edge definition and using Klebanoff's normal intermittency factor. The convective heat-transfer rate correlation formula used in the BL and BLSSW solutions includes a transition correction. The BLSSW and VSL solutions show the expected influence of vorticity interaction, but the VSL solution predicts heating rates that are approximately 30% lower than that given by the BLSSW solution. These differences are approximately the same as those obtained in the region of strong vorticity interaction for the previously discussed perfect gas solutions. For the present problem, these differences are not excessive and are generally to be expected when comparing different numerical techniques using different turbulence models. For the laminar flow region, the differenct solution procedures are in excellent agreement.

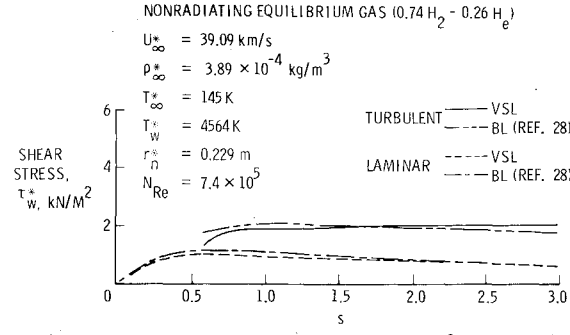

Fig. 7 Wall shear stress distribution for a 40° hyperboloid.

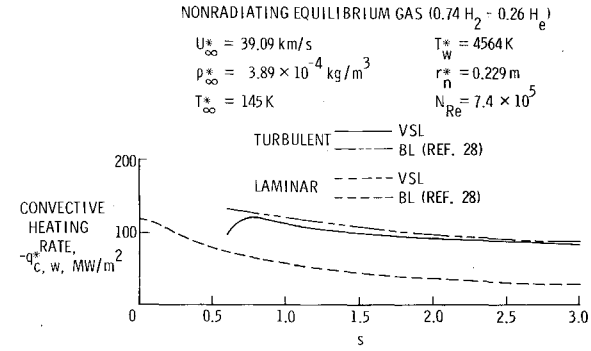

Fig. 8 Heating-rate distribution for a 40° hyperboloid.

VSL solution results are prsented in Figs. 7 and 8 for a 40° half-angle hyperboloid for freestream conditions corresponding to a typical Jovian entry trajectory point. Wall shear-stress and convective heating-rate distributions are compared with the solution obtained using the BL analysis of Bartlett and Kendall.[28] The inviscid constant entropy edge conditions for this BL solution were determined using the TFD procedure of Ref. 21. With the exception of the region near the point of instantaneous transition from laminar to turbulent flow, the wall shear-stress distributions for both laminar and turbulent flow show differences of less than ±5% except in the immediate vicinity of the transition point. Vorticity interaction is not a significant factor for this case except at greater distances downstream. Turbulent VSL solutions for radiating gas mixtures in chemical equilibrium are presented in Refs. 8, 11, and 29.

Concluding Remarks

Numerical solutions for the viscous-shock-layer equations for both laminar and turbulent flows are presented. These solutions compare favorably with inviscid flowfield solutions in the predominantly inviscid outer portion of shock layer. Favorable comparisons with boundary-layer solutions are obtained for the predominantly viscous inner portion of the shock layer both near the nose and far downstream where vorticity interaction is negligible. In flow regions where vorticity interaction is strong, the viscous-shock-layer solutions appear to be more satisfactory.

First-order boundary-layer theory with corrections for streamline swallowing appears to overpredict boundary-layer and displacement thicknesses. For turbulent flow, this results in an apparent overprediction of skin friction and heat transfer if vorticity interaction is strong. This behavior is the result of the implied nonvanishing normal gradients at the edge of the boundary layer when longitudinal entropy gradients are considered.

Experimental data are needed for hypersonic turbulent flows over blunt bodies to assess the accuracy of the present numerical solution procedure and to determine the validity of mixing length turbulence models in the presence of strong vorticity interaction.

Turbulence modeling techniques that are independent of conventional boundary-layer thickness parameters are needed for both the present method of analysis and for numerical solution of the Navier-Stokes equations.

References

[1]Moss, J. N., Anderson, E.C., and Bolz, C.W., Jr., "Viscous-Shock-Layer Solutions With Radiation and Ablation Injection for Jovian Entry," AIAA Paper 75-671 Denver, Colorado, 1975.

[2]Davis, R.T., "Numerical Solution of the Hypersonic Viscous Shock-Layer Equations," *AIAA Journal*, Vol. 8, May 1970, pp. 843-851.

[3]Davis, R.T., "Hypersonic Flow of a Chemically Reacting Binary Mixture Past a Blunt Body," AIAA Paper 70-805, Los Angeles Calif., June-July 1970.

[4]Moss, J.N., "Reacting Viscous-Shock-Layer Solutions With Multicomponent Diffusion and Mass Injection," NASA TR-411, 1974.

[5]Moss, J.N., "Stagnation and Downstream Viscous-Shock-Layer Solutions With Radiation and Coupled Ablation Injection," AIAA Paper 74-73, Washington, D.C., 1974.

[6]Eaton, R.R. and Larson, D.E., "Laminar and Turbulent Viscous Shock Layer Flow in the Symmetry Planes of Bodies at Angle of Attack," AIAA Paper 74-599, June 1974.

[7]Anderson, E.C. and Moss, J.N., "Numerical Solution of the Viscous-Shock-Layer Equations for Hypersonic Turbulent Flow of a Perfect Gas About Blunt Axially Symmetric Bodies," School of Engineering, Old Dominion University, Norfolk, Virginia, TR 74-T3, July 1974.

[8]Anderson, E.C. and Moss, J.N., "Viscous-Shock-Layer Solutions for Turbulent Flow of Radiating Gas Mixtures in Chemical Equilibrium," NASA TM X-72764, 1975.

[9]Bird, R.B., Stewart, W.E., and Lightfoot, E.N., *Transport Phenomena*, Wiley, N.Y., 1960.

[10]Dorrance, W.H., *Viscous Hypersonic Flow*, McGraw-Hill, N.Y., 1962.

[11]Anderson, E.C., Moss, J.N., and Sutton, K., "Turbulent Viscous-Shock-Layer Solutions With Strong Vorticity Interaction," AIAA Paper 76-120, Washington, D.C., Jan. 1976.

[12]Stroud, C.W., and Brinkley, Kay L., "Chemical Equilibrium of Ablation Materials Including Condensed Species," NASA TN D-5391, 1969.

[13]Esch, D.D., Siripong, A., Pike, R.W., "Thermodynamic Properties in Polynomial Form for Carbon, Hydrogen, Nitrogen, and Oxygen Systems From 300 to 15000°K," NASA CR-111989, 1970.

[14]McBride, B.J., Heimel, S., Ehlers, J.G., and Gordon, S., "Thermodynamics Properties to 6000 K for 210 Substances Involving the First 18 Elements," NASA SP-3001, 1963.

[15]Esch, D.D., Pike, R.W., Engel, Carl D., Farmer, R.C., and Balhoff, J.F., "Stagnation Region Heating of a Phenolic-Nylon Ablator During Return From Planetary Missions," NASA CR-112026, 1971.

[16]Wilke, C.R., "A Viscosity Equation for Gas Mixtures," *Journal of Chemical Physics*, Vol. 18, April 1950, pp. 517-519.

[17]Clauser, F. H., "The Turbulent Boundary Layer," *Advances in Applied Mathematics*, of Vol. IV H.L. Dryden and Th. von Karman, eds., Academic Press, Inc., 1956, pp. 1-51.

[18]Klebanoff, P.S., "Characteristics of Turbulence in a Boundary Layer With Zero Pressure Gradient, NACA Rep. 1247, 1955 (supersedes NACA TN 3178).

[19]Cebeci, T., "Behavior of Turbulent Flow Near a Porous Wall With Pressure Gradient," *AIAA Journal*, Vol. 8, Dec. 1970, pp. 2152-2156.

[20]Inouye, M., Rakich, J., and Lomax, H., "A Description of Numerical Methods and Computer Programs for Two-Dimensional and Axisymmetric Supersonic Flow Over Blunt Nosed and Flared Bodies," NASA TN D-2970, Aug. 1965.

[21]Sutton, K., "Coupled Nongray Radiating Flow About Planetary Entry Bodies," *AIAA Journal*, Vol. 12, Aug. 1974, pp. 1099-1105.

[22]Anderson, E.C., and Lewis, C.H., "Laminar or Turbulent Boundary-Layer Flows of Perfect Gases or Reacting Gas Mixtures in Chemical Equilibrium," NASA CR-1893, 1971.

[23]Mayne, A.W., Jr. and Dyer, D.F., "Comparisons of Theory and Experiment for Turbulent Boundary Layers on Simple Shapes at Hypersonic Conditions," *Proceedings of the 1970 Heat Transfer and Fluid Mechanics Institute*, Stanford University Press, Stanford, Calif., 1970, pp. 168-188.

[24]Blottner, F.G., "Finite Difference Methods of Solution of the Boundary-Layer Equations," *AIAA Jouranl*, Vol. 8, Feb. 1970, pp. 193-205.

[25]Price, S.M. and Harris, J.E., "Computer Program for Solving Compressible Nonsimilar Boundary-Layer Equations for Laminar, Transitional, or Turbulent Flows of a Perfect Gas," NASA TM X-2458, 1972.

[26]Van Dyke, M., "A Review and Extension of Second-Order Hypersonic Boundary-Layer Theory," *Rarefield Gas Dynamics, Fluid Symposium Supplement 2*, Vol. II, Academic Press, New York, 1963.

[27]Edquist, C.T., "A Technique for Predicting Shock Induced Vorticity Effects During Venus Entry," Martin-Marietta Corp., Denver Divison, Denver, Colorado, R-70-48671-006, Aug. 1970.

[28]Bartlett, E.P. and Kendall, R.M., "Nonsimilar Solution of the Multicomponent Laminar Boundary Layer by an Integral Matrix Method," Aerotherm Corp., Palo Alto, California, Aerotherm Report No. 66-7, Part III, March 14, 1967.

[29]Moss, J. N., Anderson, E.C., and Bolz, C.W., Jr., "Aerothermal Environment for Jovian Entry Probes," AIAA Paper 76-469, Sand Diego, California, July 1976.